

# FlashEdit: Decoupling Speed, Structure, and Semantics for Precise Image Editing

Junyi Wu<sup>1\*</sup> Zhiteng Li<sup>1\*</sup> Haotong Qin<sup>2</sup> Xiaohong Liu<sup>1</sup> Linghe Kong<sup>1</sup> Yulun Zhang<sup>1†</sup> Xiaokang Yang<sup>1</sup>

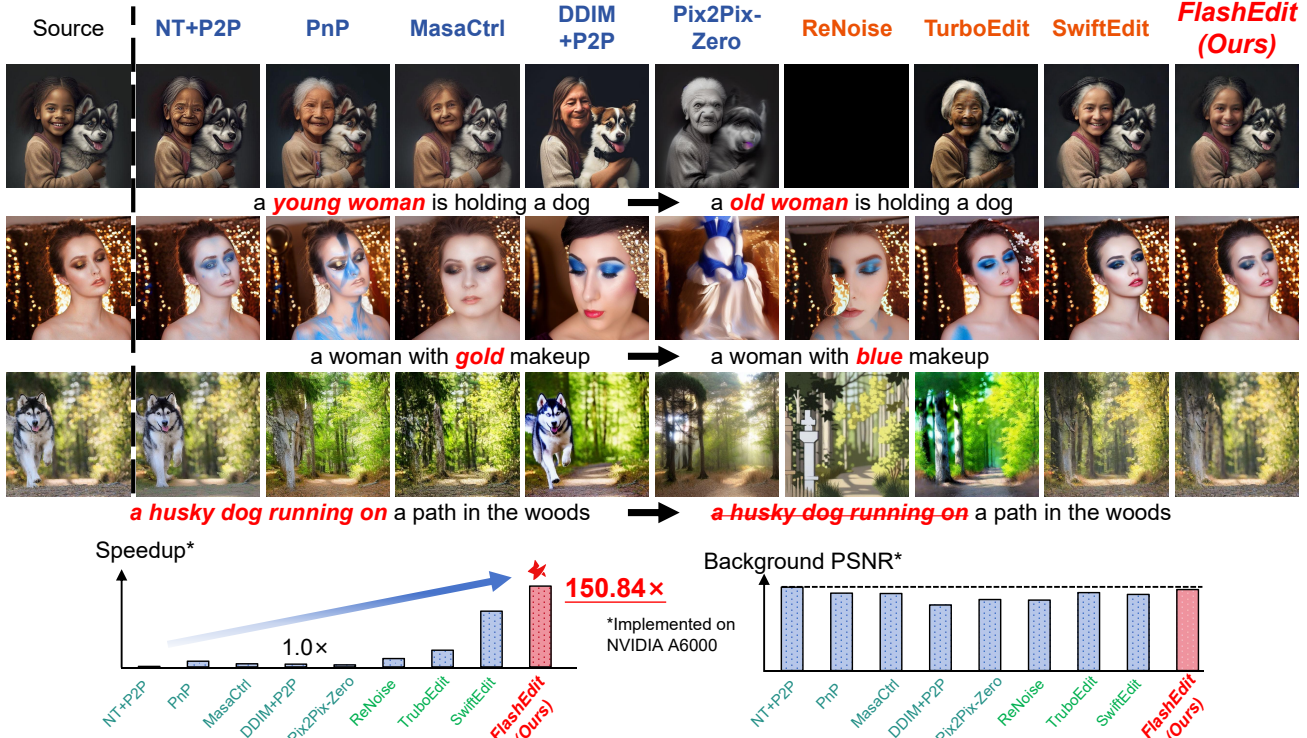


Figure 1. FlashEdit produces superior visual results for text-guided image editing, addressing background instability and semantic entanglement with an over 150 $\times$  speedup against DDIM (Song et al., 2020b) + P2P (Hertz et al., 2022).

## Abstract

Text-guided image editing with diffusion models has achieved remarkable quality but suffers from prohibitive latency. We introduce **FlashEdit**, a novel framework designed for high-fidelity, real-time image editing. Its efficiency and precision stem from three key innovations: (1) a **Cycle-Consistent One-Step Inversion (COSI)** pipeline that establishes a bijective mapping to ensure manifold alignment; (2) a **Background Shield (BG-Shield)** technique that guarantees background preservation via structural self-attention intervention; and (3) a **Sparsified Spatial Cross-**

**Attention (SSCA)** mechanism that ensures precise edits by suppressing semantic leakage. Extensive experiments demonstrate that FlashEdit maintains superior consistency while performing edits in under 0.2 seconds, achieving an over 150 $\times$  speedup.

## 1. Introduction

Text-guided image editing with diffusion models (Brooks et al., 2023; Dong et al., 2023) has demonstrated remarkable capabilities, allowing users to perform complex semantic modifications with high fidelity. The standard methodology is built upon a two-stage inversion-denoising pipeline: an initial inversion process maps a source image to its corresponding noise latent, which is then progressively denoised to generate the edited output according to a target prompt (Ju

<sup>1</sup>Shanghai Jiao Tong University <sup>2</sup>ETH Zürich. Correspondence to: Yulun Zhang <yulun100@gmail.com>.

et al., 2023; Cao et al., 2023). The objective is to achieve high fidelity in both content preservation and target prompt alignment, which often necessitates a computationally intensive, multi-step process.

Recent research has pursued several distinct strategies to improve accuracy and speed. To tackle the latency of the multi-step denoising process, methods based on model distillation have been proposed to enable editing in a faster way (Deutch et al., 2024). These approaches must carefully address challenges such as mismatched noise statistics and insufficient editing strength that arise when adapting multi-step frameworks to fast samplers (Mokady et al., 2023b; Miyake et al., 2025). To improve edit precision and prevent semantic leakage into the background, another category of work modifies the model’s internal mechanisms, primarily by re-weighting or replacing attention maps to ensure the edit is spatially constrained (Fang et al., 2024; Xu et al., 2024). Recognizing that the final edit quality is highly dependent on the starting point, other approaches focus on refining the inversion technique itself (Ju et al., 2023). These methods aim to find a more accurate initial latent vector, with recent insights revealing that separating the objectives of content preservation and edit fidelity can yield significant performance gains and speedups (Wang et al., 2025c).

However, these existing methods approach speed and quality as a trade-off rather than as interconnected components of a singular, complex control problem. They offer partial solutions like accelerating the sampler at the cost of inversion fidelity, or preserving the background without addressing the precision of the foreground edit. This results in a fragmented landscape of techniques that fail to deliver a solution that is simultaneously fast, robust, and precise. A truly practical editing framework requires a more holistic methodology that addresses control at every level of editing.

To address this multifaceted challenge, we introduce a novel editing methodology that establishes control at three progressively finer levels of granularity. At the foundational level, we tackle the macro-problem of **temporal control**. At the foundational level, we tackle the macro-problem of **manifold alignment**. We propose a **Cycle-Consistent One-Step Inversion (COSI)** pipeline, built upon a bijective loop strategy, which conquers the prohibitive latency of prior work while maintaining high reconstruction fidelity. With this temporal control established, we address the meso-level problem of **spatial control**. Our **Background Shield (BG-Shield)** mechanism provides structural integrity by performing a surgical intervention in the self-attention layers. It uses a background memory and foreground-core querying to create a hard separation between edited and unedited regions, guaranteeing background stability. Finally, with speed and structure secured, we target the micro-level problem of **semantic control**. We develop **Sparsified Spatial Cross-Attention (SSCA)**, a refinement of the cross-attention mechanism that prunes irrelevant text tokens pre-softmax, ensuring the edit is guided by a clean, unambiguous semantic signal. Each component logically builds upon the last, forming a cohesive solution (Figure 1). Our main contributions can be summarized as follows:

- We propose a novel, multi-level methodology for image editing that cohesively integrates control over three distinct levels: the temporal latency of the pipeline, the spatial structure of the image, and the semantic content of the edit with an over  $150\times$  speedup compared to prior multi-step methods.
- At the temporal and geometric level, we introduce the **Cycle-Consistent One-Step Inversion (COSI)** pipeline, which establishes a bijective mapping between the image and noise latents to ensure alignment with the generator’s specific manifold.
- At the spatial level, we propose **Background Shield (BG-Shield)**, a structural intervention in self-attention that uses memory caching and soft recomposition with attention feathering to enforce pixel-perfect background preservation, ensuring the structural integrity of the edit.
- At the semantic level, we develop **Sparsified Spatial Cross-Attention (SSCA)**, a cross-attention mechanism that performs pre-softmax token pruning. This provides the final layer of fine-grained control, eliminating attribute bleeding and enabling precise edits with complex text prompts.

## 2. Related Works

### 2.1. Diffusion Models

Recent advances in image synthesis have been largely driven by diffusion models (Peebles & Xie, 2023; Kulikov et al., 2024), which have become a leading paradigm for generating high-fidelity images from text. The core mechanism involves an iterative denoising process that progressively refines a random noise vector into a coherent image conditioned on a text prompt. A landmark contribution in this area is Stable Diffusion (Rombach et al., 2021), a Latent Diffusion Model (LDM) (Rombach et al., 2022) that performs the computationally intensive denoising process in a lower-dimensional latent space, making the technology widely accessible. Parallel to this, Flow Matching models like Flux (Labs, 2024) maps noise to an image via a more direct, straight-line trajectory, representing a different theoretical foundation for high-quality generative modeling.

To mitigate the high computational cost of these iterative models, various acceleration techniques have been proposed.

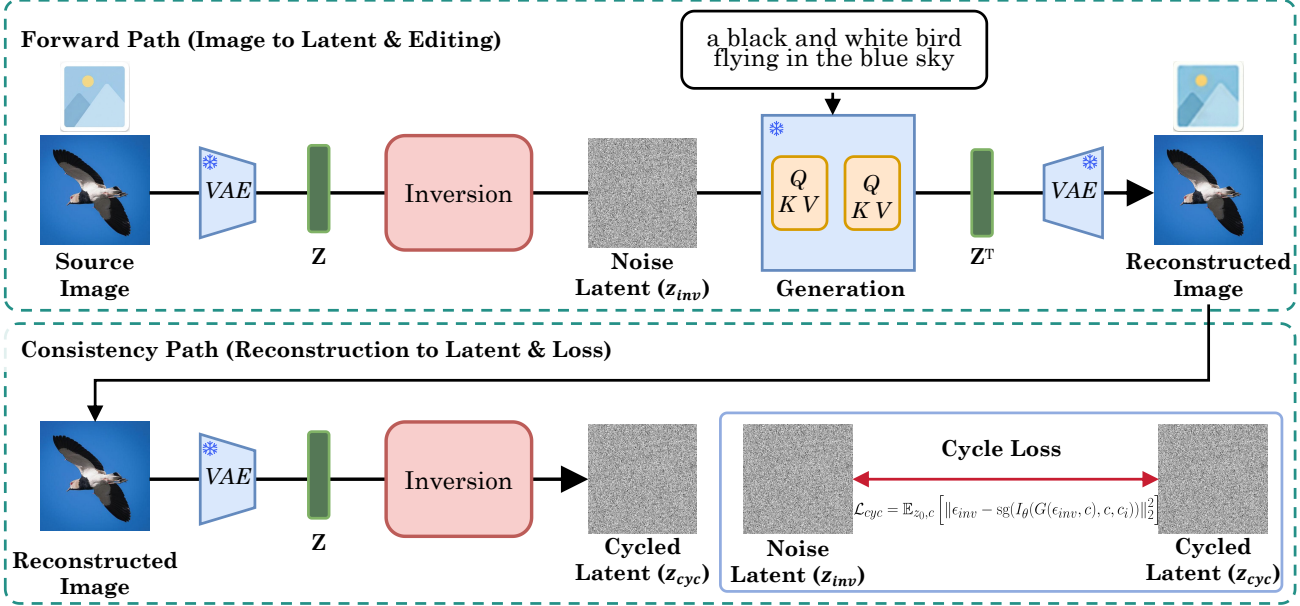


Figure 2. Overview of our **One-Step Inversion-and-Editing framework**, which introduces a direct image conditioning branch, trained via a two-stage “Anchor-and-Refine” strategy that uses direct supervision for synthetic data (Stage 1) and a teacher-student objective for real images (Stage 2).

Model quantization (Li et al., 2024a;b; 2025b; Yan et al., 2025b), cache mechanism (Xu et al., 2025; Pan et al., 2025), sparse attention (Li\* et al., 2025), pruning (Wang et al., 2025a; Yan et al., 2025a), and distillation (Hinton et al., 2015; Nguyen et al., 2025) are general acceleration techniques for deep learning model. In diffusion models, specifically, one primary category is *model quantization* (Li et al., 2025a), which reduces memory footprint and computational load by converting full-precision model weights and activations into lower-bit representations. Post-Training Quantization (PTQ) is a particularly popular training-free approach in this domain. Another category involves *cache mechanisms* (Liu et al., 2025b; Ma et al., 2024; Liu et al., 2025a), which enhance inference efficiency by exploiting temporal redundancy. These methods reuse intermediate features computed at earlier denoising steps to avoid redundant calculations in later steps. While effective in isolation, recent work like QuantCache (Wu et al., 2025) demonstrates a unified framework can yield greater gains.

## 2.2. Editing Models

The task of editing real images with pre-trained generative models introduces the fundamental challenge of *inversion*: finding a latent representation that can faithfully reconstruct a given source image. This problem was first extensively studied in the context of Generative Adversarial Networks (GAN) Inversion (Wang et al., 2022; Zhu et al., 2020; 2016). In comparison, **DDIM Inversion** (Song et al., 2020b) provides a deterministic method to find a corresponding noise latent for a source image. Once this latent is obtained, vari-

ous editing mechanisms are employed during the denoising process to apply the desired changes. A prominent family of methods focuses on *attention control*, where the cross-attention maps between text and image are manipulated. For example, to change a “photo of a red car” to a “blue car,” Prompt-to-Prompt (Hertz et al., 2022) identifies the attention weights corresponding to the word “red” and replaces them with those for “blue,” preserving the attention for “car” and the background. Another powerful technique is *feature injection*, exemplified by Plug-and-Play (PnP) (Zhang et al., 2021). To preserve the identity of a subject, PnP injects the self-attention features—which encode structure and appearance—from the source image’s generation process into the edited one. This ensures that when changing a “photo of a person” to a “photo of a person smiling,” the facial identity remains consistent. A third approach is *mask-based editing*, where methods like DiffEdit (Couairon et al., 2022) generate a mask indicating the region to be altered and then apply the denoising process only within that area. Despite these advances, a core challenge persists in perfectly disentangling the edited foreground from the unedited background. Furthermore, most of these established techniques rely on computationally intensive multi-step inference, which severely hinders real-time interaction. While recent efforts have explored accelerating editing via model distillation (Garibi et al., 2024; Deutch et al., 2024; Nguyen et al., 2025), they often compromise the delicate balance between structural preservation and semantic alignment, failing to match the fidelity of iterative solvers.

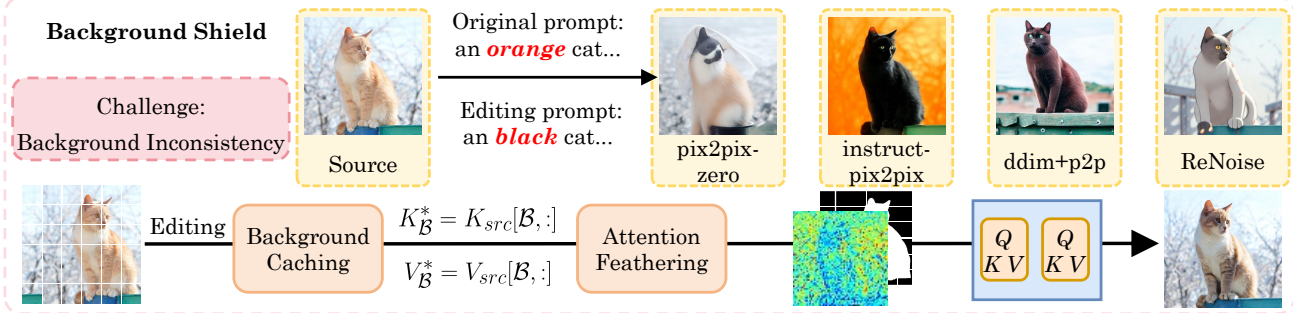


Figure 3. Overview of the Cycle-Consistent One-Step Inversion (COSI) framework. The framework consists of a **Forward Path** that maps the source image to a noise latent  $z_{inv}$  for reconstruction, and a **Consistency Path** that re-inverts the reconstruction to enforce geometric symmetry. By minimizing the **Cycle Loss** between the initial noise  $z_{inv}$  and the cycled noise  $z_{cyc}$ , COSI mathematically anchors the inversion to the generator’s manifold  $\mathcal{M}_G$ , preventing latent drift and ensuring stable, high-fidelity image editing.

### 3. Method

#### 3.1. Cycle-Consistent One-Step Inversion

##### Challenge: Manifold Misalignment and Latent Drift.

Traditional inversion for multi-step diffusion relies on iterative refinement to push the noise latent into a region that perfectly reconstructs the source image. However, in one-step generative frameworks, the solution space is extremely narrow, and the generative trajectory is highly sensitive to the initial noise distribution. While distillation-based methods (Nguyen et al., 2025) attempt to map images to noise via a teacher’s guidance, they often suffer from *manifold misalignment*. In one-step models, the generator  $G$  characterizes a precise, low-dimensional manifold  $\mathcal{M}_G$  where the generative dynamics are significantly more compressed than multi-step counterparts. In such a compressed space, the model lacks the “self-correction” capacity inherent in multi-step sampling. The predicted noise  $\epsilon_{inv}$  from heuristic distillation may yield a visually plausible reconstruction  $\hat{z}_0$  at the pixel level, but it frequently fails to reside on the exact manifold  $\mathcal{M}_G$ . This off-manifold noise introduces a hidden instability; when the latent is perturbed by a target prompt  $c_{tgt}$  for editing, this initial “manifold gap” is amplified by the one-step decoder. Without subsequent denoising steps to buffer this error, it manifests as *latent drift*. Consequently, the model exhibits catastrophic background flickering and structural collapses, as the starting point lacks the mathematical grounding required for stable, trajectory-consistent single-step denoising.

##### Motivation: From Mimicry to Bijective Manifold Anchoring.

Our key insight is that a robust inversion should not merely mimic a teacher’s noise prediction but must act as a functional, structural inverse of the generator  $G$ . In a one-step setting, where the diffusion ODE is approximated by a direct mapping, the relationship between the image latent  $z_0$  and the noise  $\epsilon$  should ideally approximate a *bijective mapping* within the generative subspace. Without such a constraint, the inversion mapping is ill-posed, often

resulting in a “many-to-one” collapse where distinct image details are erroneously mapped to identical noise regions, sacrificing both reconstructive fidelity and editability. We hypothesize that by enforcing a **Cycle-Consistency Constraint**, we can regularize the inversion network  $I_\theta$  to find the “canonical” noise latent. This canonical latent is mathematically anchored to the generator’s specific manifold, transforming the inversion-denoising path from an open-ended approximation into a self-contained, closed loop. By ensuring the inversion is “aware” of the generator’s reconstruction logic, we preserve structural invariants even under aggressive semantic shifts. This anchoring effectively restricts the inverted noise to the high-probability region of the generator’s distribution, making the editing process inherently more predictable and robust.

##### Proposed Method: Cycle-Consistent Bijective Loop.

To resolve these issues, we propose **COSI**, which moves beyond simple distillation by integrating a self-supervised alignment objective. We define the inversion mapping as  $\epsilon_{inv} = I_\theta(z_0, c, c_i)$ , where  $c$  is the text condition and  $c_i$  is the visual adapter feature. While an initial foundational mapping is established using existing one-step training paradigms, our core contribution lies in bridging the manifold gap through the **Inversion Cycle**. Unlike previous works that treat the inversion network as a black-box regressor, COSI treats it as a symmetric partner to the generator, aiming for a mathematical “closed loop.”

For any given reconstruction  $\hat{z}_0 = G(\epsilon_{inv}, c)$ , the cycle-consistency principle dictates that feeding this reconstructed image back into the inversion network must recover the original noise  $\epsilon_{inv}$ . We optimize  $I_\theta$  by minimizing the deviation between the initial predicted noise and the noise re-extracted from the reconstruction:

$$\mathcal{L}_{cyc} = \mathbb{E}_{z_0, c} \left[ \|\epsilon_{inv} - \text{sg}(I_\theta(G(\epsilon_{inv}, c), c, c_i))\|_2^2 \right], \quad (1)$$

where  $\text{sg}(\cdot)$  denotes the stop-gradient operation to ensure that the inversion network specifically learns to adapt to the

generator’s fixed output characteristics. Unlike traditional distillation losses that rely on an external teacher  $\phi$ ,  $\mathcal{L}_{cyc}$  provides a *geometry-aware* signal that is intrinsically tied to the generator  $G$ . This objective forces  $I_\theta$  to learn the precise inverse geometry of the one-step manifold by verifying its own predictions through the generator’s lens. By closing this loop, COSI ensures that the inverted noise resides within the high-fidelity region of the generative space, providing a robust, “invertible” starting point that maintains absolute background integrity even under complex semantic edits.

### 3.2. Background Shield

**Challenge: Background Inconsistency.** A critical challenge in localized image editing is maintaining strict background consistency. We observe that even with precise masks, many methods fail at this task. For instance, in Figure 3 when performing a seemingly simple edit such as changing “an orange cat” to “a black cat”, the background suffers from unintended alterations, leading to shifts in color, lighting, or style. We identify the root cause of this instability as the inherent nature of the self-attention mechanism. As a global operator that computes all-to-all relationships between image tokens, it allows the strong semantic signal from the foreground edit to propagate and contaminate the background features, undermining the goal of a truly localized edit.

**Motivation.** Having identified the global nature of self-attention as the cause of this background inconsistency, our motivation is to move beyond merely scaling influences and propose a direct structural intervention. To achieve background stability, a hard constraint that structurally isolates the background from the editing process is required. We introduce **Background Shield (BG-Shield)**, a method designed to enforce this consistency by replacing the background’s feature computation with a direct recall from a “background memory”.

**Proposed Method.** Shown in Figure 3, BG-Shield operates as a two-pass mechanism within self-attention layers. Let  $X \in \mathbb{R}^{S \times D}$  be the input feature sequence, and let a binary mask  $M \in \{0, 1\}^S$  define the foreground indices  $\mathcal{F}$  and background indices  $\mathcal{B}$ .

**Background Memory Caching.** During a forward pass with the source prompt  $c_{src}$ , we compute the Key and Value matrices,  $K_{src}, V_{src}$ . We then extract and cache the background-specific key-value pairs:

$$K_{\mathcal{B}}^* = K_{src}[\mathcal{B}, :], \quad V_{\mathcal{B}}^* = V_{src}[\mathcal{B}, :]. \quad (2)$$

This cached memory,  $(K_{\mathcal{B}}^*, V_{\mathcal{B}}^*)$ , serves as a high-fidelity record of the original background state.

**Soft Recomposition with Attention Feathering.** During the editing pass with the target prompt  $c_{tgt}$ , we compute

new queries, keys, and values  $(Q_{tgt}, K_{tgt}, V_{tgt} \in \mathbb{R}^{S \times d_k})$ . We then construct a spatially-aware, full key-value set,  $K_{full}, V_{full}$ , by combining the background memory with the current foreground features:

$$K_{full}[j, :] = \begin{cases} K_{\mathcal{B}}^*[\text{rank}_{\mathcal{B}}(j), :] & \text{if } j \in \mathcal{B} \\ K_{tgt}[j, :] & \text{if } j \in \mathcal{F} \end{cases} \quad (3)$$

$$V_{full}[j, :] = \begin{cases} V_{\mathcal{B}}^*[\text{rank}_{\mathcal{B}}(j), :] & \text{if } j \in \mathcal{B} \\ V_{tgt}[j, :] & \text{if } j \in \mathcal{F} \end{cases} \quad (4)$$

where  $\text{rank}_{\mathcal{B}}(j)$  ensures correct positional alignment.

To mitigate boundary artifacts and ensure a smooth blend, we replace the hard-masking of the original “foreground core” approach with an **Attention Feathering** mechanism. We first create a soft alpha mask  $A \in [0, 1]^S$  by applying a Gaussian blur to the binary mask  $M$ :

$$A = \text{GaussianBlur}(M, \text{kernel\_size} = \sigma) \quad (5)$$

This alpha mask creates a “transition zone”. This zone softly connects the editing foreground, where the mask value is close to one, and the preserved background, where the mask value is close to zero.

Next, we compute the full attention output,  $H_{edit} \in \mathbb{R}^{S \times d_k}$ , where all queries  $Q_{tgt}$  attend to the recomposed key-value set  $(K_{full}, V_{full})$ :

$$H_{edit} = \text{softmax} \left( \frac{Q_{tgt} K_{full}^T}{\sqrt{d_k}} \right) V_{full}. \quad (6)$$

The final sparse output matrix  $H$  is then obtained by  $H_{edit}$  with our soft alpha mask  $A$ :

$$H = A \odot H_{edit} \quad (7)$$

where  $\odot$  denotes element-wise multiplication.

### 3.3. Sparsified Spatial Cross-Attention

#### Challenge: Semantic Entanglement in Image Editing.

A key challenge in precise image editing is *semantic entanglement*, where textual attributes are not cleanly bound to their intended objects. As demonstrated in Figure 4, when changing “a cat with yellow eyes” to “a cat with green eyes,” standard cross-attention often fails to isolate the edit region. This failure stems from the inherent *all-to-all* nature of the softmax function in vanilla cross-attention layers. Since every pixel is forced to compute a probability distribution across all text tokens, a highly salient but spatially irrelevant token (e.g., “green”) can dominate the attention map. This leads to two critical artifacts: *edit attenuation*, where the intended change is suppressed by structural tokens, and *attribute leakage*, where the new attribute bleeds onto surrounding unedited regions (e.g., an unnatural green tint on

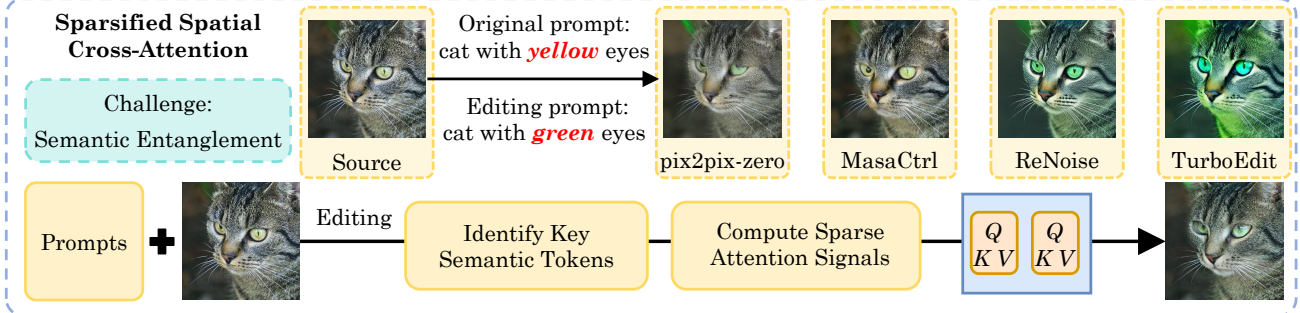


Figure 4. Illustration of our **Sparsified Spatial Cross-Attention (SSCA)** method resolving *semantic entanglement*. The top row demonstrates how standard attention fails on precise edits, resulting in edit attenuation and attribute leakage. The bottom row details our SSCA mechanism, which prevents this by computing attention only over a subset of relevant text tokens to ensure a clean edit.

Table 1. Comprehensive comparison of editing quality, evaluating background preservation and CLIP similarity across various methods.

Method		Background Preservation				CLIP Similarity	
Inverse	Editing	PSNR $\uparrow$	LPIPS $\times 10^3 \downarrow$	MSE $\times 10^4 \downarrow$	SSIM $\times 10^2 \uparrow$	Whole $\uparrow$	Edited $\uparrow$
DDIM	P2P	17.87	208.80	219.88	71.14	25.01	22.44
NT-Inv	P2P	27.03	60.67	35.86	84.11	24.75	21.86
DDIM	MasaCtrl	22.17	106.62	86.97	79.67	23.96	21.16
Direct Inversion	MasaCtrl	22.64	87.94	81.09	81.33	24.38	21.35
DDIM	P2P-Zero	20.44	172.22	144.12	74.67	22.80	20.54
Direct Inversion	P2P-Zero	21.53	138.98	127.32	77.05	23.31	21.05
DDIM	PnP	22.28	113.46	83.64	79.05	25.41	22.55
Direct Inversion	PnP	22.46	106.06	80.45	79.68	25.41	22.62
ReNoise(SDXL)		20.85	176.84	51.78	72.44	24.41	21.88
TurboEdit		22.51	107.27	9.32	80.09	25.49	21.82
SwiftEdit		23.31	71.54	6.18	82.25	25.56	21.91
<b>FlashEdit</b>		25.33	62.25	4.28	83.32	25.51	22.29
<b>FlashEdit(w/ GT masks)</b>		25.28	62.43	4.33	83.02	25.58	22.32

the cat’s fur). The root cause is that the softmax normalization allows unrelated semantic signals to interfere with each other spatially.

#### Motivation: Pre-emptive Semantic Disentanglement.

Based on this diagnosis, we contend that semantic concepts must be disentangled *before* the non-linear softmax allows them to compete globally. Our motivation is to implement a **pre-emptive disentanglement** strategy that restricts the receptive field of each pixel in the textual domain. By forcing the model to attend only to a clean, task-relevant subset of tokens for a given spatial region, we can eliminate attribute bleeding at its source. We introduce **Sparsified Spatial Cross-Attention (SSCA)**, which treats text attention not as a global competition, but as a localized, sparse retrieval process that preserves the high-frequency semantic boundaries of the edit.

**Proposed Method: Sparse-to-Dense Integration.** As illustrated in Figure 4, the SSCA mechanism redefines text-guided guidance through a three-stage pipeline of identifica-

tion, pruning, and structural integration.

**Identifying Key Semantic Tokens.** Rather than processing the entire prompt  $y$ , we first localize the most significant textual cues for the edit region defined by mask  $M$ . We compute the aggregate similarity between the foreground image queries  $Q_{l,\mathcal{F}}$  and the full set of text keys  $K_y$ . Specifically, for each text token  $j$ , we compute a relevance score  $R_j = \sum_{i \in \mathcal{F}} (Q_{l,i} \cdot K_{y,j}^T) / \sqrt{d}$ . We then select the *top-k* text key-value pairs with the highest scores, denoted as  $(K_y^k, V_y^k)$ . This operation acts as a high-pass semantic filter, discarding irrelevant background tokens (e.g., “background”, “sky”) that might otherwise dilute the foreground edit.

**Computing Focused Sparse Attention Signal.** With the pruned semantic subset, we compute a focused attention result  $A_{\text{sparse}}$  exclusively for the foreground queries  $Q_{l,\mathcal{F}}$ .

The sparse attention for a foreground pixel  $i \in \mathcal{F}$  is com-

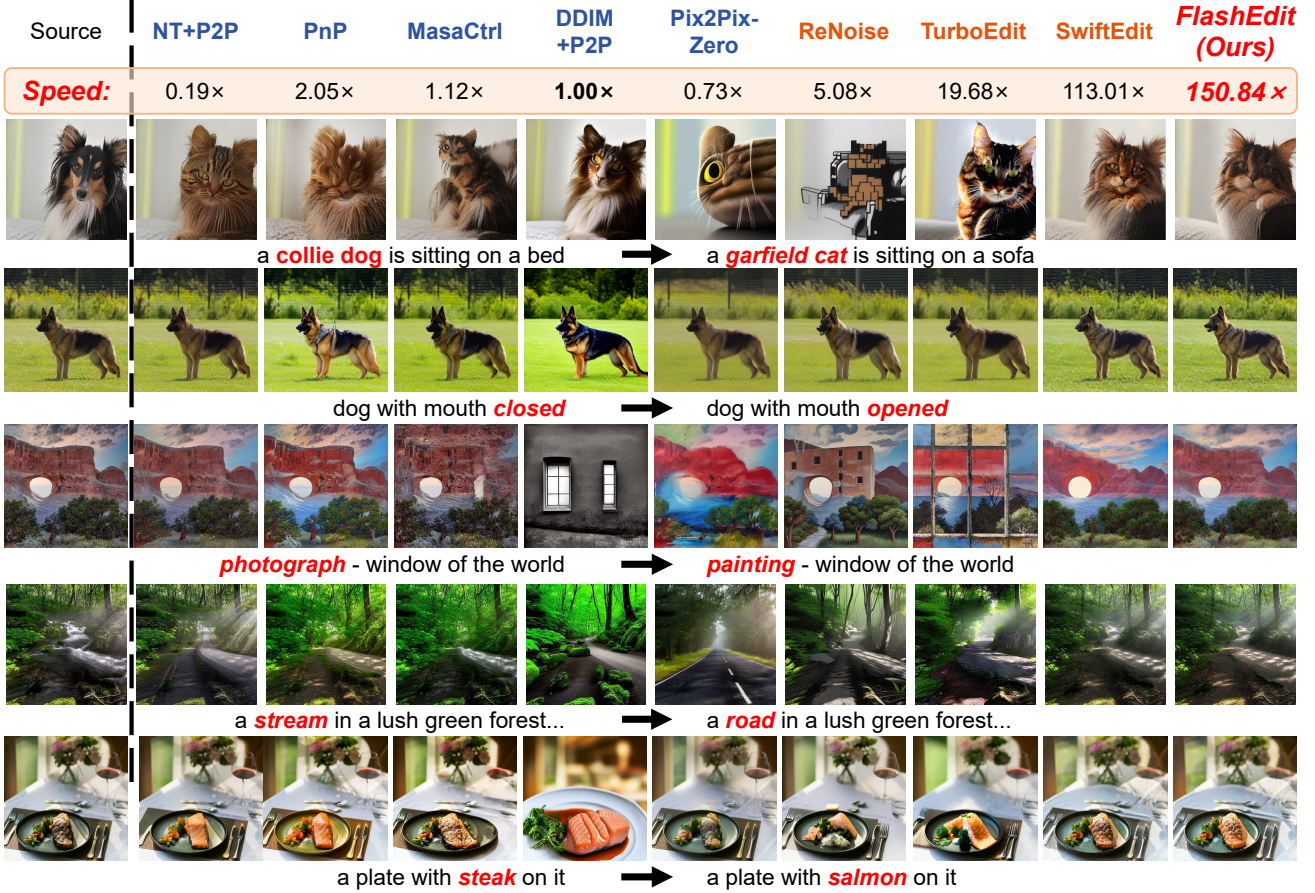


Figure 5. Qualitative comparison of editing results. Each row corresponds to a unique editing task, with the source image displayed in the first column and the source/target prompts listed below.

puted as:

$$A_{\text{sparse},i} = \text{softmax} \left( \frac{Q_{l,i}(K_y^k)^T}{\sqrt{d}} \right) V_y^k. \quad (8)$$

By restricting the denominator of the softmax to only  $k$  relevant tokens, we ensure that the semantic energy of the target attribute (e.g., “green”) is concentrated on the correct spatial coordinates without being leaked into the global feature mean.

**Structural Integration via Zero-Masking.** To ensure that the target prompt has strictly zero influence on the unedited background, we scatter the sparse results into a zero-initialized full-size attention matrix  $A_{\text{SSCA}} \in \mathbb{R}^{S \times d}$ :

$$A_{\text{SSCA}}[i,:] = \begin{cases} A_{\text{sparse}}[\text{rank}_{\mathcal{F}}(i),:] & \text{if } i \in \mathcal{F} \\ \mathbf{0} & \text{if } i \notin \mathcal{F} \end{cases}. \quad (9)$$

This structural zero-masking ensures a clean decoupling between foreground semantics and background textures. The final output is integrated into the model through the standard

residual connection, resulting in an attribute-faithful edit that remains spatially confined to the masked region.

## 4. Experiment

### 4.1. Experimental Settings

**Implementation Details.** We implement our framework and architecture in PyTorch inspired by (Wang et al., 2025b; Nguyen et al., 2025; Chen et al., 2025), using the Adam optimizer (Kingma & Ba, 2014). We evaluate our method on the PieBench benchmark (Zhang et al., 2021), which features 700 samples across 10 editing types. We report metrics along two primary axes. As for **Background Preservation**, We compute PSNR (Huynh-Thu & Ghanbari, 2008), LPIPS (Zhang et al., 2018), MSE and SSIM (Wang et al., 2004) on the unedited regions to measure fidelity to the source image. As for **Semantic Alignment**, We report CLIP-Whole (Radford et al., 2021) for prompt-image alignment and CLIP-Edited (Radford et al., 2021) for alignment within masked edit regions. Experiments were conducted on a NVIDIA A6000 GPU.

**Table 2. Ablation Study on Core Model Components.** We evaluate the contribution of each module by measuring the impact on background preservation and semantic similarity (CLIP Score). The final row represents our full method.

Components			Background Preservation				CLIP Similarity	
COSI	BG-Shield	SSCA	PSNR $\uparrow$	LPIPS $\times 10^3 \downarrow$	MSE $\times 10^4 \downarrow$	SSIM $\times 10^2 \uparrow$	Whole $\uparrow$	Edited $\uparrow$
✓	-	-	23.38	92.29	6.58	80.01	24.17	21.28
✓	✓	-	24.69	75.28	4.96	81.95	24.80	21.28
✓	✓	✓	25.33	62.25	4.28	83.32	25.51	22.29

**Baselines.** We compare our method against state-of-the-art baselines. For **multi-step** methods, we evaluate Prompt-to-Prompt (P2P) (Hertz et al., 2022), MasaCtrl (Cao et al., 2023), Pix2Pix-Zero (Parmar et al., 2023), and Plug-and-Play (PnP) (Zhang et al., 2021), paired with inversion techniques like DDIM (Song et al., 2020a), Null-text Inversion (NT-Inv) (Mokady et al., 2023a), and Direct Inversion (Ju et al., 2023). For **few-steps** methods, we compare against Renoise (Garibi et al., 2024), TurboEdit (Deutch et al., 2024) and SwiftEdit (Nguyen et al., 2025).

## 4.2. Quantitative Analysis

As shown in Table 1, our method establishes a new state-of-the-art for accelerated editing. FlashEdit significantly outperforms recent **few-step methods** like ReNoise (Garibi et al., 2024) and TurboEdit (Deutch et al., 2024) across all reported metrics. Crucially, it also achieves quality on par with, and in several metrics superior to, top-performing but prohibitively slow **multi-step methods**. This high fidelity is delivered with an extraordinary efficiency gain of over **150 $\times$**  (Table 3). Furthermore, an experiment using ground-truth (GT) masks reveals a negligible performance difference, confirming the high accuracy of our self-guided masking mechanism.

## 4.3. Qualitative Analysis

Visual comparisons in Figure 5 reinforce our quantitative findings. The outputs from FlashEdit consistently exhibit high semantic fidelity to the target prompt while maintaining pristine background integrity, avoiding the “bleeding” artifacts common in other methods. In contrast, other baselines often display noticeable quality degradation or fail to preserve background details. FlashEdit is unique in providing both state-of-the-art visual quality and the real-time performance that multi-step methods lack.

## 4.4. Ablation Studies

To validate the contribution of each component in our framework, we conduct a comprehensive ablation study, with the results presented in Table 2. Our baseline, consisting of the **COSI** pipeline alone, establishes a strong foundation by ensuring bijective manifold alignment. Integrating **BG-**

**Table 3.** Efficiency comparison of individual editing methods, with the denoising steps and speedup factor for each specific combination.

Method		Denoising Steps	Speedup
Inverse	Editing		
DDIM	P2P		<b>1.00<math>\times</math></b>
NT-Inv	P2P		0.19 $\times$
DDIM	MasaCtrl		1.12 $\times$
Direct Inversion	MasaCtrl	Multi-steps	0.88 $\times$
DDIM	P2P-Zero		0.73 $\times$
Direct Inversion	P2P-Zero		0.73 $\times$
DDIM	PnP		2.06 $\times$
Direct Inversion	PnP		2.03 $\times$
ReNoise(SDXL)		Few-steps	5.08 $\times$
TurboEdit			19.68 $\times$
SwiftEdit		One-step	113.01 $\times$
<b>FlashEdit(Ours)</b>			<b>150.84<math>\times</math></b>

**Shield** brings a marked improvement across background preservation metrics, confirming its effectiveness in isolating background features. The final addition of **SSCA** further boosts metrics. It substantially enhances semantic alignment, evidenced by a large increase in the CLIP-Edited score, which validates our pre-softmax token pruning strategy. **SSCA** also improves reconstruction quality, suggesting a synergistic effect where cleaner textual guidance benefits the entire process. This demonstrates that all three components are critical and work in concert to achieve the final state-of-the-art performance of **FlashEdit**.

## 5. Conclusion

This paper introduces **FlashEdit**, a new paradigm for text-guided image editing that redefines the performance standard for generative applications. We demonstrate that the long-standing trade-off between speed and quality is not fundamental but can be overcome with a holistic, multi-level control strategy. Our approach establishes geometric stability through the **COSI** pipeline for manifold-aware inversion, enforces spatial integrity with the **BG-Shield** mechanism, and secures fine-grained semantic precision via **SSCA**, transforming diffusion-based editing into a true creative tool.

## References

Brooks, T., Holynski, A., and Efros, A. A. Instructpix2pix: Learning to follow image editing instructions. In *CVPR*, 2023.

Cao, M., Wang, X., Qi, Z., Shan, Y., Qie, X., and Zheng, Y. Masactrl: Tuning-free mutual self-attention control for consistent image synthesis and editing. In *ICCV*, 2023.

Chen, Z., Zou, Z., Zhang, K., Su, X., Yuan, X., Guo, Y., and Zhang, Y. Dove: Efficient one-step diffusion model for real-world video super-resolution. In *NeurIPS*, 2025.

Couairon, G., Verbeek, J., Schwenk, H., and Cord, M. Diffedit: Diffusion-based semantic image editing with mask guidance. *arXiv preprint arXiv:2210.11427*, 2022.

Deutch, G., Gal, R., Garibi, D., Patashnik, O., and Cohen-Or, D. Turboedit: Text-based image editing using few-step diffusion models. In *SIGGRAPH Asia*, 2024.

Dong, W., Xue, S., Duan, X., and Han, S. Prompt tuning inversion for text-driven image editing using diffusion models. In *ICCV*, 2023.

Fang, J., Jiang, H., Wang, K., Ma, Y., Jie, S., Wang, X., He, X., and Chua, T.-S. Alphaedit: Null-space constrained knowledge editing for language models. *arXiv preprint arXiv:2410.02355*, 2024.

Garibi, D., Patashnik, O., Voynov, A., Averbuch-Elor, H., and Cohen-Or, D. Renoise: Real image inversion through iterative noising. In *ECCV*, 2024.

Hertz, A., Mokady, R., Tenenbaum, J., Aberman, K., Pritch, Y., and Cohen-Or, D. Prompt-to-prompt image editing with cross attention control. *arXiv preprint arXiv:2208.01626*, 2022.

Hinton, G., Vinyals, O., and Dean, J. Distilling the knowledge in a neural network. *arXiv preprint arXiv:1503.02531*, 2015.

Huynh-Thu, Q. and Ghanbari, M. Scope of validity of psnr in image/video quality assessment. *Electronics Letters*, 2008.

Ju, X., Zeng, A., Bian, Y., Liu, S., and Xu, Q. Direct inversion: Boosting diffusion-based editing with 3 lines of code. *arXiv preprint arXiv:2310.01506*, 2023.

Kingma, D. P. and Ba, J. Adam: A method for stochastic optimization. *arXiv preprint arXiv:1412.6980*, 2014.

Kulikov, V., Kleiner, M., Huberman-Spiegelglas, I., and Michaeli, T. Flowedit: Inversion-free text-based editing using pre-trained flow models. *arXiv preprint arXiv:2412.08629*, 2024.

Labs, B. F. Flux. <https://github.com/black-forest-labs/flux>, 2024.

Li, J., Xu, J., Huang, S., Chen, Y., Li, W., Liu, J., Lian, Y., Pan, J., Ding, L., Zhou, H., et al. Large language model inference acceleration: A comprehensive hardware perspective. *arXiv preprint arXiv:2410.04466*, 2024a.

Li, J., Xu, J., Li, S., Huang, S., Liu, J., Lian, Y., and Dai, G. Fast and efficient 2-bit llm inference on gpu: 2/4/16-bit in a weight matrix with asynchronous dequantization. In *ICCAD*, 2024b.

Li\*, X., Li\*, M., Cai, T., Xi, H., Yang, S., Lin, Y., Zhang, L., Yang, S., Hu, J., Peng, K., Agrawala, M., Stoica, I., Keutzer, K., and Han, S. Radial attention:  $\mathcal{O}(n \log n)$  sparse attention with energy decay for long video generation. *arXiv preprint arXiv:2506.19852*, 2025.

Li, Z., Li, H., Wu, J., Liu, K., Kong, L., Chen, G., Zhang, Y., and Yang, X. Dvd-quant: Data-free video diffusion transformers quantization. *arXiv preprint arXiv:2505.18663*, 2025a.

Li, Z., Yan, X., Zhang, T., Qin, H., Xie, D., Tian, J., zhongchao shi, Kong, L., Zhang, Y., and Yang, X. Arbllm: Alternating refined binarizations for large language models. In *ICLR*, 2025b.

Liu, J., Zou, C., Lyu, Y., Chen, J., and Zhang, L. From reusing to forecasting: Accelerating diffusion models with taylorseers. *arXiv preprint arXiv:2503.06923*, 2025a.

Liu, J., Zou, C., Lyu, Y., Chen, J., and Zhang, L. From reusing to forecasting: Accelerating diffusion models with taylorseers. *arXiv preprint arXiv:2503.06923*, 2025b.

Ma, X., Fang, G., and Wang, X. Deepcache: Accelerating diffusion models for free. In *CVPR*, 2024.

Miyake, D., Iohara, A., Saito, Y., and Tanaka, T. Negative-prompt inversion: Fast image inversion for editing with text-guided diffusion models. In *WACV*, 2025.

Mokady, R., Hertz, A., Aberman, K., Pritch, Y., and Cohen-Or, D. Null-text inversion for editing real images using guided diffusion models. In *CVPR*, 2023a.

Mokady, R., Hertz, A., Aberman, K., Pritch, Y., and Cohen-Or, D. Null-text inversion for editing real images using guided diffusion models. In *CVPR*, 2023b.

Nguyen, T.-T., Nguyen, Q., Nguyen, K., Tran, A., and Pham, C. Swiftedit: Lightning fast text-guided image editing via one-step diffusion. In *CVPR*, 2025.

Pan, J., Xu, J., Zhou, Y., and Dai, G. Specdiff: Accelerating diffusion model inference with self-speculation. *arxiv preprint 2509.13848*, 2025.

Parmar, G., Kumar Singh, K., Zhang, R., Li, Y., Lu, J., and Zhu, J.-Y. Zero-shot image-to-image translation. In *SIGGRAPH*, 2023.

Peebles, W. and Xie, S. Scalable diffusion models with transformers. In *ICCV*, 2023.

Radford, A., Kim, J. W., Hallacy, C., Ramesh, A., Goh, G., Agarwal, S., Sastry, G., Askell, A., Mishkin, P., Clark, J., et al. Learning transferable visual models from natural language supervision. In *ICML*, 2021.

Rombach, R., Blattmann, A., Lorenz, D., Esser, P., and Ommer, B. High-resolution image synthesis with latent diffusion models. *arXiv preprint arXiv:2112.10752*, 2021.

Rombach, R., Blattmann, A., Lorenz, D., Esser, P., and Ommer, B. High-resolution image synthesis with latent diffusion models. In *CVPR*, 2022.

Song, J., Meng, C., and Ermon, S. Denoising diffusion implicit models. *arXiv:2010.02502*, October 2020a. URL <https://arxiv.org/abs/2010.02502>.

Song, J., Meng, C., and Ermon, S. Denoising diffusion implicit models. *arXiv preprint arXiv:2010.02502*, 2020b.

Wang, H., Xu, J., Pan, J., Zhou, Y., and Dai, G. Specprune-vla: Accelerating vision-language-action models via action-aware self-speculative pruning. *arxiv preprint 2509.05614*, 2025a.

Wang, J., Gong, J., Zhang, L., Chen, Z., Liu, X., Gu, H., Liu, Y., Zhang, Y., and Yang, X. OSDFace: One-step diffusion model for face restoration. In *CVPR*, 2025b.

Wang, J., Hu, J., Ma, X., Ma, H., Wei, X., and Wu, E. Image editing with diffusion models: A survey. *arXiv preprint arXiv:2504.13226*, 2025c.

Wang, T., Zhang, Y., Fan, Y., Wang, J., and Chen, Q. High-fidelity gan inversion for image attribute editing. In *CVPR*, 2022.

Wang, Z., Bovik, A., Sheikh, H., and Simoncelli, E. Image quality assessment: from error visibility to structural similarity. *TIP*, 2004.

Wu, J., Li, Z., Hui, Z., Zhang, Y., Kong, L., and Yang, X. Quantcache: Adaptive importance-guided quantization with hierarchical latent and layer caching for video generation. In *ICCV*, 2025.

Xu, J., Pan, J., Zhou, Y., Chen, S., Li, J., Lian, Y., Wu, J., and Dai, G. Specee: Accelerating large language model inference with speculative early exiting. In *ISCA*, 2025.

Xu, Y., Tang, F., Cao, J., Zhang, Y., Kong, X., Li, J., Deusser, O., and Lee, T.-Y. Headrouter: A training-free image editing framework for mm-dits by adaptively routing attention heads. *arXiv preprint arXiv:2411.15034*, 2024.

Yan, X., Li, Z., Zhang, T., Kong, L., Zhang, Y., and Yang, X. Recalkv: Low-rank kv cache compression via head reordering and offline calibration. *arXiv preprint arXiv:2505.24357*, 2025a.

Yan, X., Zhang, T., Li, Z., and Zhang, Y. Progressive binarization with semi-structured pruning for llms. *arXiv preprint arXiv:2502.01705*, 2025b.

Zhang, K., Li, Y., Zuo, W., Zhang, L., Van Gool, L., and Timofte, R. Plug-and-play image restoration with deep denoiser prior. *TPAMI*, 2021.

Zhang, R., Isola, P., Efros, A. A., Shechtman, E., and Wang, O. The unreasonable effectiveness of deep features as a perceptual metric. In *CVPR*, 2018.

Zhu, J., Shen, Y., Zhao, D., and Zhou, B. In-domain gan inversion for real image editing. In *ECCV*, 2020.

Zhu, J.-Y., Krähenbühl, P., Shechtman, E., and Efros, A. A. Generative visual manipulation on the natural image manifold. In *ECCV*, 2016.